Schroeder, F., Perlmutter, J. F., Glaser, M., & Vagelos, P. R. (1976a) *J. Biol. Chem. 251*, 5015.
Schroeder, F., Holland, J. F., & Vagelos, P. R. (1976b) *J. Biol. Chem. 251*, 6739.
Schroeder, F., Holland, J. F., & Vagelos, P. R. (1976c) *J. Biol. Chem. 251*, 6747.
Shinitzky, M., & Inbar, M. (1976) *Biochim. Biophys. Acta 433*, 133.
Shinitzky, M., Dianous, A.-C., Gitler, C., & Weber, G. (1971) *Biochemistry 10*, 2106.
Spencer, R. D., & Weber, G. (1970) *J. Chem. Phys. 52*, 1654.
Tombaccini, D., Ruggieri, S., Fallini, A., & Mugani, G. (1980) *Biochem. Biophys. Res. Commun. 96*, 1109.
Vaughan, D. J., & Keough, K. M. (1979) *FEBS Lett. 47*, 158.
Warren, L. (1959) *J. Biol. Chem. 234*, 1971.
Weltzien, H. U. (1975) *Z. Naturforsch., C: Biosci 30C*, 785.

Unifying Description of the Effect of Membrane Proteins on Lipid Order. Verification for the Melittin/Dimyristoylphosphatidylcholine System†

Fritz Jähnig,* Horst Vogel, and Lüder Best

ABSTRACT: The effect of melittin on lipid order in dimyristoylphosphatidylcholine bilayers is investigated by means of Raman spectroscopy and fluorescence anisotropy using diphenylhexatriene as fluorescence probe. In the fluid lipid phase, the Raman results indicate a slight increase in the conformational order of the lipid chains, and the fluorescence anisotropy results indicate a considerable increase in the rigid-body orientational order of the lipid chains. These results are contrasted with the reported decrease of the deuterium magnetic resonance order parameter. A consistent interpretation of the complete set of experimental data is presented according to which proteins induce a tilt of the preferred axes of lipid orientation and increase the orientational order with respect to these axes. The values of the tilt angle and the orientational order parameter at the surface of proteins are determined from the experimental data within a continuum model of lipid–protein interaction. The same values are obtained for melittin, Ca/Mg-ATPase, and cytochrome *c* oxidase, suggesting that different membrane proteins affect the lipid order in the same way.

A large body of experimental data on the effect of proteins on lipid order in membranes has been accumulated during the past few years. However, no consensus has been attained as to whether proteins in a fluid membrane cause an ordering or a disordering of the lipids. The confusion arises from the disagreement of results obtained by different experimental techniques. On the one hand, electron spin resonance (ESR),[1] fluorescence anisotropy (FA), and Raman spectroscopy indicate that proteins increase the lipid order. On the other hand, deuterium magnetic resonance (^{2}H NMR) indicates that proteins decrease the lipid order.

A consistent interpretation of these experimental results has been proposed previously (Jähnig, 1979), requiring that proteins induce a tilt of the preferred axes of lipid orientation and increase the lipid orientational order with respect to these tilted axes. In the present paper, this concept is elaborated quantitatively within the framework of a continuum model of lipid–protein interaction (Owicki et al., 1978; Jähnig, 1981). Here a protein molecule imposes at its surface boundary conditions upon the tilt angle of the preferred axes and the lipid orientational order parameter. With increasing distance from the protein the perturbation of lipid order falls off exponentially with a characteristic length given by the coherence length of lipid order. Within this model, the experimental data representing different averages of the spatially varying lipid order can be evaluated for the boundary values of the tilt angle and the orientational order parameter.

The determination of the boundary order parameter is exemplified by the system melittin in dimyristoylphosphatidylcholine bilayers on the basis of Raman and FA results presented. If FA data from the literature for two other proteins, Ca/Mg-ATPase and cytochrome *c* oxidase, are evaluated in the same way, a striking similarity among different proteins is found. The boundary tilt angle is determined for Ca/Mg-ATPase and cytochrome *c* oxidase, for which the necessary ^{2}H NMR data are available. The result again indicates a similarity amont different proteins in their effect on lipid order.

Materials and Methods

Chemicals. DMPC was purchased from Fluka. No impurities were detected by thin-layer chromatography. Melittin was from Mack (Illertissen, BRD) and was purified by gel filtration through a Sephadex G-100 column in the presence of 10^{-3} M HCl. Diphenylhexatriene (DPH) was obtained from EGA-Chemie (Steinheim, BRD).

Sample Preparation for X-ray and Raman Measurements. A 10-mg sample of DMPC and an appropriate amount of melittin were dissolved in 100 μL of freshly distilled 2-chloroethanol. After addition of 2 mL of benzene, the mixture was freeze-dried. Buffer (10^{-3} M Tris-HCl and 10^{-4} M EDTA, pH 7.4) was added to the dry samples to obtain a water/lipid weight ratio of 1/1. The membrane preparations were incubated for 2 h at 35 °C, then transferred to thin-walled glass capillaries, and centrifuged for 10 min at 50000*g*

† From the Max-Planck-Institut für Biologie, 7400 Tübingen, BRD. *Received May 5, 1982.* This work was supported by the Deutsche Forschungsgemeinschaft through Ja 243.

[1] Abbreviations: ^{2}H NMR, deuterium magnetic resonance; ESR, electron spin resonance; FA, fluorescence anisotropy; DPH, diphenylhexatriene; tPnA, *trans*-parinaric acid; DMPC, dimyristoylphosphatidylcholine; DPPC, dipalmitoylphosphatidylcholine; P(PO)PC, 1-palmitoyl-2-palmitoleoylphosphatidylcholine; POPC, 1-palmitoyl-2-oleoylphosphatidylcholine; DOPC, dioleoylphosphatidylcholine; Tris, tris(hydroxymethyl)aminomethane; EDTA, ethylenediaminetetraacetic acid.

0006-2960/82/0421-6790$01.25/0

and 4 °C. Samples with low water content for X-ray measurements were obtained by incubating freeze-dried lipid or lipid/melittin membranes for 4 h at 80 °C in a saturated water vapor atmosphere. The water content was determined by weighing the hydrated samples before and after drying in a desiccator at 10^{-3} torr and 60 °C.

X-ray and Raman Measurements. These were performed as described by Jähnig et al. (1979) and Vogel & Jähnig (1981), respectively. The conditions for the Raman measurements were 514.5 nm excitation wavelength, 400 mW, and 5 cm^{-1} slit widths.

The intensity of the investigated Raman band at 1127 cm^{-1} was normalized to the intensity of the band at 717 cm^{-1} which originates from the C–N stretch vibration in the lipid polar head group and is invariant with temperature and addition of melittin. The band intensities were approximated by the band peak heights I_0.

Sample Preparation for Fluorescence Measurements. DMPC vesicles were prepared by tip sonication in buffer (10^{-3} M Tris-HCl and 10^{-4} M EDTA, pH 7.4, for anisotropy measurements and 5×10^{-2} M sodium hydrogen phosphate, 10^{-1} M NaCl, and 10^{-4} M EDTA, pH 7.4, for quenching measurements) for 45 min at 30 °C, followed by centrifugation at 12000*g* for 10 min at 20 °C. For anisotropy measurements, a desired amount of DPH dissolved in dioxane was added and the mixture incubated for 90 min at 30 °C. The DMPC/DPH mole ratio was 1000, the final lipid concentration 4×10^{-4} M, and the dioxane concentration below 0.4 vol %. Dispersions of lipid vesicles without fluorescence labels but with the same concentration of dioxane as above were used to correct for light scattering. Appropriate amounts of a 4×10^{-4} M solution of melittin in buffer were added to the lipid dispersions followed by incubation for 15 min at 30 °C. All measurements were made within 3 h after the addition of melittin. Samples of DMPC/melittin with L/P = 10 prepared in the same way as for the Raman measurements except for the high lipid concentration were shown to yield the same results for the fluorescence anisotropy.

Fluorescence Measurements. These were performed with a Perkin-Elmer MPF-3 spectrometer. For anisotropy measurements, quartz polarizing prisms were inserted in the excitation and emission light path. For circumvention of monochromator corrections, a multiwave plate quartz wedge depolarizer was inserted between the analyzer and the emission monochromator. The sample was irradiated with vertically polarized light at 360 nm for DPH-FA. The vertically and horizontally polarized fluorescence intensity components, $I_\parallel$ and $I_\perp$, were recorded at 430 nm. $I_\parallel$ and $I_\perp$ of lipid dispersions without fluorescence labels were subtracted from the signals of the labeled membranes. The light scattering contribution to $I_\parallel$ was less than 5% of the total intensity. The steady-state fluorescence anisotropy r_s was determined as

$$r_s = \frac{I_\parallel - I_\perp}{I_\parallel + 2I_\perp}$$

For the measurements of tryptophan fluorescence quenching, DPH from a stock solution in dioxane was added to a stirred dispersion of DMPC/melittin vesicles. The intensities of the tryptophan fluorescence of melittin and of the DPH fluorescence were recorded alternatingly, irradiating at 280 and 360 nm and observing at 330 and 430 nm, respectively. The rationale was to increase the concentration of the quencher molecules DPH by exploiting the slow partitioning of DPH molecules into the lipid bilayer. The instantaneous concentration of incorporated DPH was determined via the increase of the fluorescence of DPH (excited at 360 nm) upon incorporation into the lipid bilayer and by assuming complete incorporation at infinitely long times.

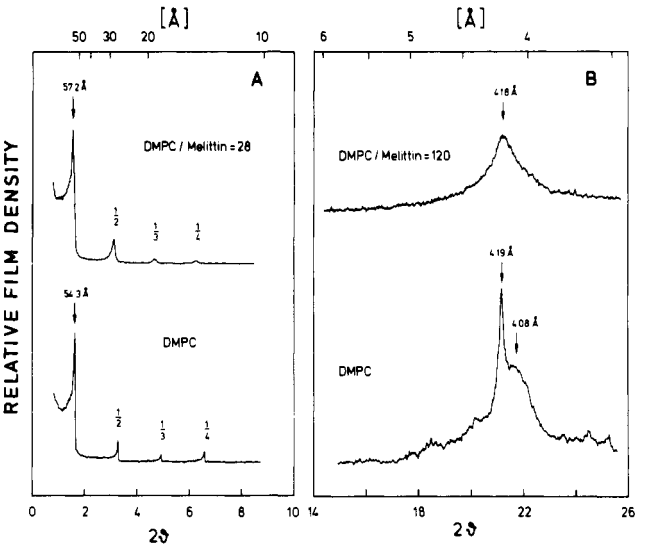

FIGURE 1: (A) X-ray diffraction pattern at low scattering angles 2ϑ and 5 °C of pure DMPC with 13 wt % H_2O and of a DMPC/melittin mixture with L/P = 28 and 21 wt % H_2O. The ratios indicate the order of the Bragg peaks and the numbers above the first order peak the lamellar repeat distance. (B) Diffraction pattern at high scattering angles and 5 °C of pure DMPC and of a DMPC/melittin mixture with L/P = 120, 50 wt % buffer. The numbers above the peaks indicate the lattice constants.

Experimental Results

X-ray Diffraction. Since melittin is known to have lytic properties (Sessa et al., 1969; Dawson et al., 1978), the existence of bilayers in the presence of melittin was studied. Figure 1A shows X-ray diffraction patterns at low scattering angles for DMPC with and without melittin. The sharp Bragg peaks indicate the presence of bilayers at least up to this melittin concentration. In Figure 1B diffraction patterns at high scattering angles are shown for pure DMPC bilayers and DMPC/melittin bilayers. The result for pure DMPC at 5 °C is characteristic for the $L\beta'$ phase of phosphatidylcholines in which the lipid chains are located laterally on a centered rectangular lattice and tilted with respect to the membrane normal (Janiak et al., 1976). In the case of the melittin-containing bilayers at 5 °C only one broadened diffraction peak is found, indicating that the lipid chains form a hexagonal lattice with considerable disorder.

Raman Spectroscopy. Raman spectra in the range 700–1200 cm^{-1} are shown in Figure 2 for pure DMPC bilayers and DMPC/melittin bilayers with L/P = 10, at three different temperatures. The intensity of the band at 1127 cm^{-1} is plotted in Figure 3A as a function of temperatue for the lipid/melittin mole ratios of 100, 40, 25, and 10 and in Figure 3B as a function of melittin concentration at two temperatures below and above the ordered-fluid phase transition temperature T_t. The transition temperature T_t remains unaltered in the presence of melittin up to the highest melittin concentration investigated. This is in agreement with the calorimetric result for L/P = 50 (Mollay, 1976). The so-called pretransition at 13 °C is suppressed by low concentrations of melittin. In the ordered phase, the intensity of the 1127-cm^{-1} band decreases linearly with increasing melittin concentration at low melittin concentration and levels off around L/P = 25. This signals either saturation of the DMPC bilayer with melittin, as suggested by studies of the binding of melittin to DMPC vesicles

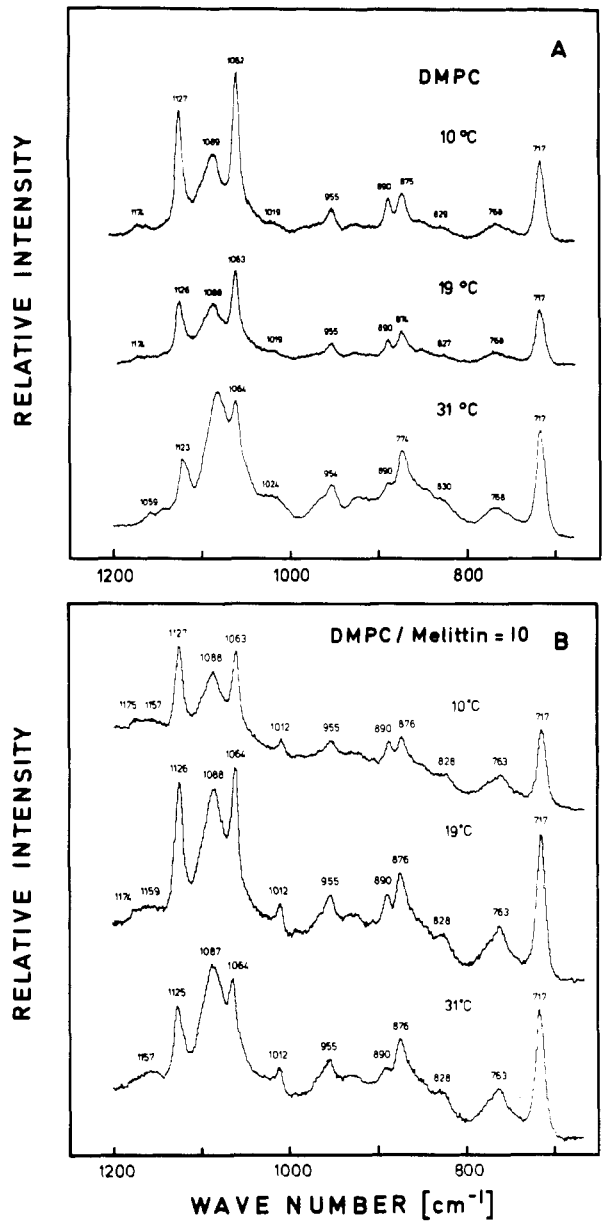

FIGURE 2: Raman spectra of the region 700–1200 cm^{-1} at different temperatures for (A) pure DMPC and (B) a DMPC/melittin mixture with L/P = 10, 50 wt % buffer.

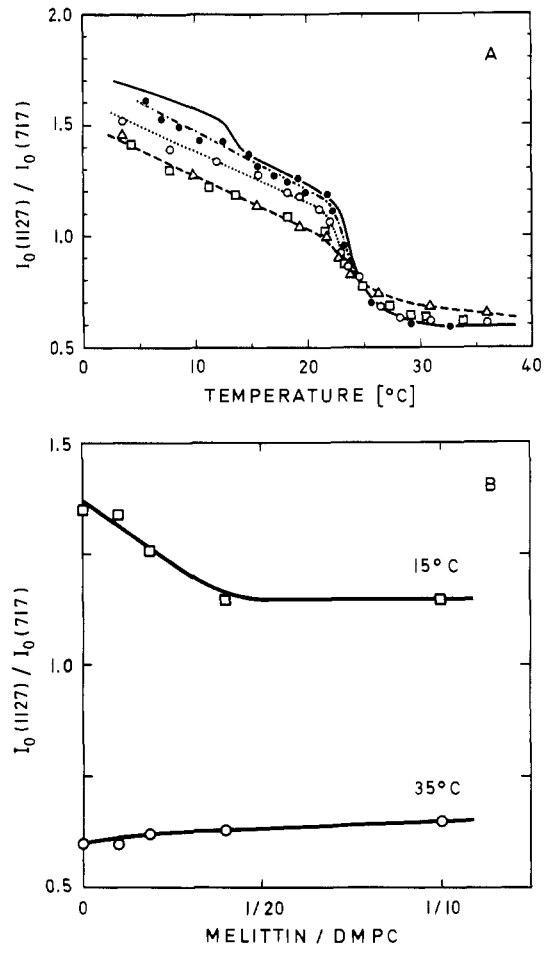

FIGURE 3: Variation of the intensity of the 1127-cm^{-1} band (A) with temperature for pure DMPC (—) and for the DMPC/melittin mole ratios of 100 (●), 40 (○), 25 (□), and 10 (△) and (B) with the melittin/DMPC mole ratio at 15 (□) and 35 (○) °C.

(Vogel, 1981), or the overlap of perturbations from neighboring melittin molecules which reduces the perturbation per melittin molecule, or a superposition of both effects. In the fluid phase, the intensity of the 1127-cm^{-1} band increases slightly with increasing melittin concentration.

Our result for high melittin concentration, L/P = 10, below and above T_t agrees with that of Lavialle et al. (1980). These authors, however, found a more complex temperature dependence in the region of the phase transition.[2] The increase of the intensity of the 1127-cm^{-1} band by melittin in the fluid phase parallels the result for other proteins investigated, the myelin proteolipid apoprotein (Curatolo et al., 1978), gramicidin A (Chapman et al., 1977; Weidekamm et al., 1977; Susi et al., 1979), and lysozyme (Lippert et al., 1980).

Fluorescence Anisotropy. The steady-state FA of DPH in pure DMPC bilayers and in DMPC/melittin bilayers with L/P = 10 is presented in Figure 4A as a function of temperature. Figure 4B shows the dependence of the DPH anisotropy on the melittin concentration at two temperatures below and above the phase transition. The transition temperature remains constant upon addition of melittin to DMPC, as was observed in the Raman measurements. In the ordered phase, melittin has no effect on the DPH anisotropy. In the fluid phase, however, the DPH anisotropy is increased considerably by melittin. The anisotropy levels off around L/P $\approx$ 25, as in the case of the Raman measurements.

The constancy of the transition temperature and the increase of the DPH anisotropy upon addition of melittin above T_t observed here are at variance with the findings of Galla et al. (1978). Our results for melittin, however, are in qualitative agreement with those for other proteins, including Ca/Mg-ATPase (Gomez-Fernandez et al., 1979; Seelig et al., 1981), cytochrome *c* oxidase (Kawato et al., 1980; Hoffmann et al., 1981), bacteriorhodopsin (Heyn et al., 1981), and gramicidin A (Hoffmann et al., 1981).

Recently, the reliability of DPH as a probe of lipid chain order has been questioned by proposing a "vertical" motion of DPH in the bilayer (Engel & Prendergast, 1981). Therefore as a control of the DPH measurements we have employed another probe, *trans*-parinaric acid (tPnA), to measure the anisotropy. The charged polar group of tPnA assures a lo-

[2] This discrepancy between the results of Lavialle et al. (1980) and ours may result from different preparations of melittin. Commercially available melittin contains traces of phospholipase A_2. We have taken great care to prepare phospholipase-free melittin so that by thin-layer chromatography we could not detect any decomposition of lipid at the end of the Raman measurements. When phospholipase A_2, however, was added to the lipid/melittin samples, a complex alteration of the phase transitional behavior was observed.

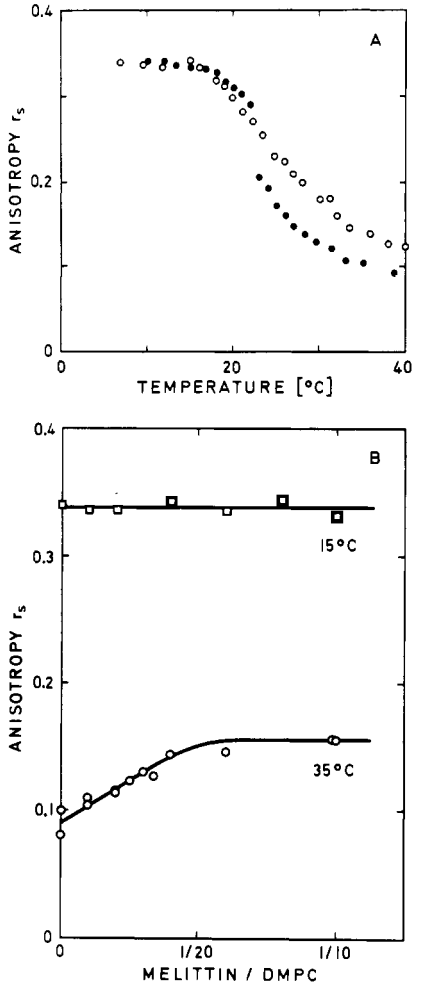

FIGURE 4: (A) Temperature dependence of the steady-state fluorescence anisotropy r_s of DPH in pure DMPC (●) and DMPC/melittin vesicles with L/P = 10 (○) and (B) variation of r_s with the melittin/DMPC mole ratio at 15 (□) and 35 °C (○).

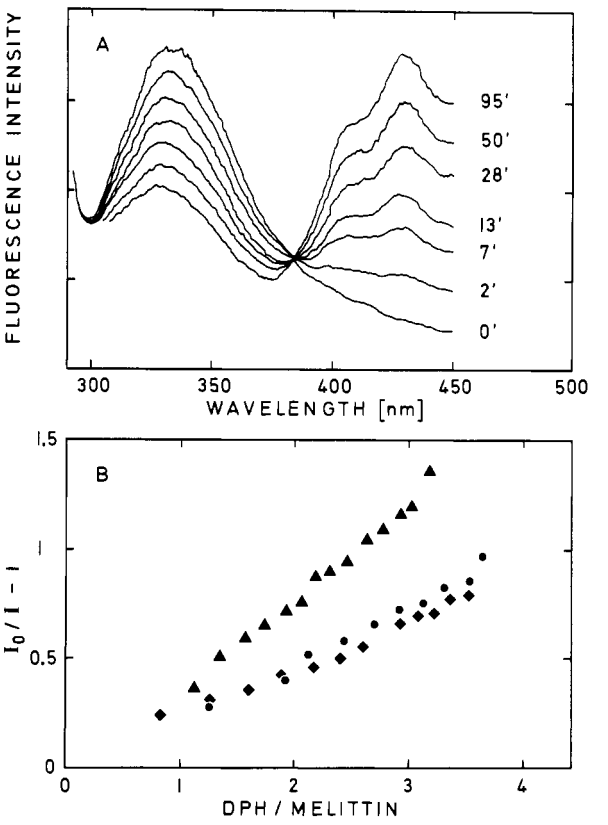

FIGURE 5: Quenching of the tryptophan fluorescence of melittin by DPH. (A) Emission spectra at different times (minutes) after the addition of DPH to DMPC/melittin vesicles with L/P = 133 at 30 °C, total mole ratio DPH/melittin = 2, and excitation at 280 nm. (B) Decrease of the tryptophan fluorescence as a function of the concentration of membrane-incorporated DPH at 18 (♦), 23 (●), and 30 °C (▲). I and I_0 are the fluorescence intensities at 330 nm of samples with and without DPH incorporated, respectively.

cation in the bilayer similar to that of the lipids. The preliminary results indicate that the steady-state anisotropy of tPnA is systemically higher than that of DPH, due to the shorter fluorescence lifetime of tPnA (Wolber & Hudson, 1981), but that the relative increase of the anisotropy with the concentration of melittin at 35 °C is similar to that of the DPH anisotropy. This supports the notion that DPH has a location in the bilayer similar to that of tPnA. It may be mentioned that a considerable increase of the tPnA anisotropy has also been observed with the M-13 coat protein (Kimelman et al., 1979).

Quenching of Melittin Fluorescence. The constancy of the DPH anisotropy in the ordered phase may be ascribable to either of two reasons: Melittin does not affect the order of the surrounding lipids, or melittin perturbs the lipid order in its neighborhood with exclusion of DPH molecules from these perturbed regions. The proximity of DPH to melittin molecules was investigated by means of fluorescence energy transfer from the tryptophanyl residue of melittin to DPH. Figure 5A shows the emission spectra of DMPC/melittin bilayers with L/P = 133 for different times after the addition of DPH, i.e., different concentrations of DPH in the bilayers (see Materials and Methods). In Figure 5B we plotted the decrease of the tryptophan fluorescence against the DPH concentration. A theoretical treatment of the Förster mechanism for energy transfer in two dimensions under the assumption of a constant distance between interacting melittin and DPH molecules predicts a straight line in this plot (Wolber & Hudson, 1979). Independent of any detailed interpretation, Figure 5B indicates that the energy transfer efficiencies below and above T_t are of the same order of magnitude, suggesting that DPH molecules have no preference for either an ordered or fluid environment. The same conclusion has been derived previously from studies of the partitioning of DPH in lipid mixtures (Lentz et al., 1976). Hence DPH detects the lipid order including the neighborhood of melittin below and above T_t, and the FA studies with DPH below T_t indicate melittin does not alter the lipid order in the ordered phase.

Model for Lipid–Protein Interaction

The experimental data will be evaluated within a continuum model for lipid–protein interaction (Owicki et al., 1978; Jähnig, 1981). The lipid order is characterized by the orientational order of the hydrocarbon chain segments which is described by two quantities for each segment: (i) the preferred axis of orientation and (ii) the orientational order parameter characterizing the strength of the orientation with respect to this preferred axis:

$$S = \left\langle \frac{3\cos^2\theta - 1}{2} \right\rangle \qquad (1)$$

Here θ is the angle between the instantaneous orientation of the segment and the preferred axis, and the angular brackets denote the average over the thermal fluctuations of the segment orientation within a definite time range.

In pure lipid bilayers, the preferred axis is parallel to the membrane normal, at least in the fluid phase, and the aver-

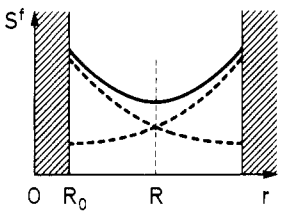

FIGURE 6: Illustration of the model for lipid–protein interaction. The dashed lines represent the perturbations of lipid order by a given protein molecule and the neighboring protein molecules, and the solid line represents the superposition of both perturbations.

aging process is achieved in nanoseconds or less as shown by FA (Kawato et al., 1977; Lakowicz et al., 1979; Wolber & Hudson, 1981) and by ^{2}H NMR (Brown et al., 1979). The corresponding order parameter is denoted S^f, the superscript indicating the average over the fast nanosecond fluctuations. The preferred axis of the fast fluctuations is often called director.

A protein present in the bilayer alters the lipid order by imposing boundary conditions on the director and on the order parameter. Let the order parameter at the protein surface be S^f_0 and the tilt angle of the director with respect to the membrane normal be θ^s_0 (the superscript s indicates slow for reasons which will become clear later). The perturbations decrease continuously from the boundary values due to the long-range character of the lipid order, until the unperturbed order parameter S^f_u and the unperturbed tilt angle $\theta^s_u = 0$ are reached. Assuming cylindrical symmetry, the decay of the order parameter S^f is given in good approximation by

$$S^f(r) = S^f_u + (S^f_0 - S^f_u)e^{-(r-R_0)/\xi} \quad (2)$$

and the decay of the tilt angle θ^s or $x^s \equiv \cos\theta^s$ by

$$x^s(r) = 1 - (1 - x^s_0)e^{-(r-R_0)/\lambda} \quad (3)$$

R_0 denotes the protein radius, and ξ and λ denote two coherence lengths for the order parameter and the director, respectively. On the basis of theoretical arguments, ξ has a pronounced temperature dependence with a maximum at the ordered-fluid transition and is of the order of 15 Å (Jähnig, 1981). Much less is known about λ; a theoretical estimate suggests λ is of comparable magnitude to ξ, but not smaller than ξ.[3] The lipid molecules located within the coherence lengths may be called boundary lipids.

Equations 2 and 3 describe the perturbation of lipid order around an isolated protein molecule. At finite protein concentrations, the perturbations from neighboring protein molecules overlap. To take this into account, we assume the protein molecules are homogeneously distributed in the membrane plane, and the protein molecules around one protein impose another cylindrical boundary condition on the lipid order, as illustrated in Figure 6. Adding the perturbations exerted by the one protein and the neighboring proteins we obtain

$$S^f(r) = S^f_u + (S^f_0 - S^f_u)[e^{-(r-R_0)/\xi} + e^{(r-2R+R_0)/\xi}] \quad (4)$$

Here R denotes the radius at the midpoint between the two boundaries and is determined by the lipid/protein mole ratio L/P via the relation

$$R^2 - R_0^2 = \frac{1}{2}\left(\frac{L}{P}\right)R_L^2 \quad (5)$$

with R_L the radius of a lipid molecule. This relation holds for a transmembrane protein spanning the two halves of the bilayer. For molecules restricted to one monolayer, the factor $^1/_2$ would have to be omitted. For $x^s(r)$ an expression analogous to eq 4 is assumed:

$$x^s(r) = 1 - (1 - x^s_0)[e^{-(r-R_0)/\lambda} + e^{(r-2R+R_0)/\lambda}] \quad (6)$$

The overlap of perturbations implies a shift of the values of S^f and x^s at the protein surface relative to the values S^f_0 and x^s_0 for an isolated protein, e.g.

$$S^f(R_0) = S^f_0 + (S^f_0 - S^f_u)e^{-2(R-R_0)/\xi} \quad (7)$$

$S^f(r)$ and $\theta^s(r)$ are defined as the local order parameter and the local tilt angle of the director, respectively. This requires that a lipid molecule stays long enough at one location to establish the average over the nanosecond fluctuations. This is actually the case since the residence time of a lipid molecule is 10^{-7} s, in the fluid phase. During times longer than the residence time the lipids undergo lateral diffusion. This gives rise to additional orientational fluctuations, namely, of the director. Averaging over these fluctuations involves averaging over the local tilt angles, taking account of the spatial variation of the local order parameters. The time required for the establishment of this average is given by the time a lipid molecule needs to diffuse from one protein molecule to another, i.e., over a distance of the order of R. For R = 40 Å, a typical value for a lipid/protein ratio of 100, and a diffusion coefficient of 10^{-8} cm^2/s, this averaging time is 10^{-5} s. Compared to the fast fluctuations which occurred in 10^{-9} s, these additional fluctuations are slow, and the tilt angle θ^s was therefore denoted slow.

The fast and slow fluctuations together lead to the total or global order parameter characterizing the strength of the

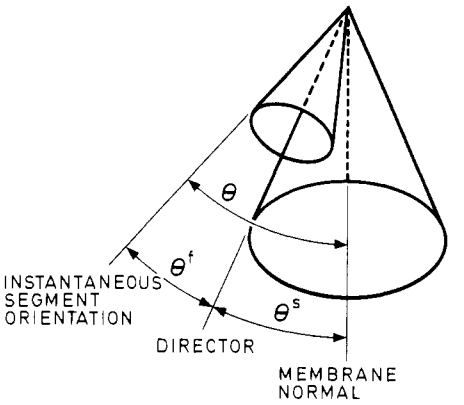

FIGURE 7: Illustration of the splitting of the angle θ, which describes the instantaneous orientation of a lipid chain segment, into a fast and a slow component, θ^f and θ^s, respectively. The angular distributions are indicated by cones.

[3] The assumption of an exponential decay of director perturbations is not trivial. In liquid crystals such perturbations decay with $1/r$, except in the case of an external magnetic field where the decay is exponential (de Gennes, 1974). For lipid bilayers, this is actually the case, since the surface pressure arising from the hydrophobic effect acts as an external field. The analogy to liquid crystals permits an estimate of the magnitude of the coherence length λ via the relation

$$\lambda = \left(\frac{K}{\Lambda S^f_u}\right)^{1/2}\left(\frac{1}{x^f_u}\right)$$

Here K is an elastic constant, $K \approx 10^{-6}$ dyn, Λ is the van der Waals interaction constant per volume, $\Lambda \approx 10^6$ ergs/cm^3 (based on $\Lambda \approx 0.6$ kcal/mol and a chain volume of 400 Å^3), and $x^f_u = \langle\cos\theta^f\rangle$ in analogy to eq 1. With $S^f_u = 0.4$ and $x^f_u = 0.7$ one obtains $\lambda \approx 20$ Å; i.e., λ is of the same order of magnitude as the order parameter coherence length ξ. Since generally, however, director perturbations require less energy than order parameter perturbations, λ is not expected to be smaller than ξ.

orientational order with respect to the total or global preferred axis, the membrane normal. The separation of the total average into a fast and a slow average corresponds to the splitting of the angle θ in eq 1 into a fast and a slow component, as illustrated in Figure 7. The total order parameter S is then given by the product of two terms involving θ^f and θ^s:

$$S = \left\langle \left\langle \frac{3\cos^2\theta^f - 1}{2} \right\rangle_f \frac{3\cos^2\theta^s - 1}{2} \right\rangle_s$$

By fast averaging the first term becomes $S^f(r)$, and calculating the slow average as a spatial average one obtains

$$S = \frac{2}{R^2 - R_0^2}\int_{R_0}^{R} S^f(r)\frac{3\cos^2\theta^s(r) - 1}{2} r\,dr$$

The integral is calculated approximately by replacing the average of the product by the product of averages to that

$$S = \overline{S^f}S^s \tag{8}$$

with

$$\overline{S^f} = \frac{2}{R^2 - R_0^2}\int_{R_0}^{R} S^f(r) r\,dr$$

and

$$S^s = \frac{2}{R^2 - R_0^2}\int_{R_0}^{R} \frac{3\cos^2\theta^s(r) - 1}{2} r\,dr$$

$\overline{S^f}$ is simply the spatial average of $S^f(r)$. S^s characterizes the strength of the orientational order of the director with respect to the membrane normal, the superscript indicating the average over the slow fluctuations arising from lateral diffusion.

Insertion of eq 4 and 6 into the integrals leads to the results

$$\overline{S^f} = S^f_u + 2\frac{\xi^2}{R^2 - R_0^2}\left[\left(1 + \frac{R_0}{\xi}\right) - 2c + \left(1 - \frac{R_0}{\xi}\right)c^2\right](S^f_0 - S^f_u) \tag{9}$$

with $c = \exp[-(R - R_0)/\xi]$ and

$$S^s = 1 - 3\frac{\lambda^2}{R^2 - R_0^2}\left\{2\left[\left(1 + \frac{R_0}{\lambda}\right) - 2c + \left(1 - \frac{R_0}{\lambda}\right)c^2 - \frac{R^2 - R_0^2}{\lambda^2}c^2\right](1 - x^s_0) - \frac{1}{4}\left[\left(1 + 2\frac{R_0}{\lambda}\right) - 2c + \left(1 - 2\frac{R_0}{\lambda}\right)c^2\right](1 - x^s_0)^2\right\} \tag{10}$$

The dependence of the two order parameters on the lipid/protein ratio is contained solely in the radius R via eq 5, whereas S^f_0 and x^s_0 are by definition independent of L/P. In the limit of low protein concentration, $R - R_0 \gg \xi$, these expressions simplify considerably, e.g.

$$\overline{S^f} = S^f_u + 4\left(\frac{P}{L}\right)\left(\frac{\xi}{R_L}\right)^2\left(1 + \frac{R_0}{\xi}\right)(S^f_0 - S^f_u)$$

Here $\overline{S^f}$ varies linearly with protein content. At higher protein concentration, $\overline{S^f}$ attains a limiting value due to the exponential term c in eq 9. This effect was studied by Hoffmann et al. (1981).

In this model, two types of lipid order are distinguished, fast and slow orientational order, and consequently the lipid–protein interaction is specified by two parameters at the lipid–protein interface: the fast orientational order parameter S^f_0 and the tilt angle θ^s_0 of the preferred axes of orientation which determines the slow orientational order. These two parameters are regarded as phenomenological quantities to be determined from experiment.[4]

Experimentally Measured Order Parameters

ESR detects the fast orientational order parameter $S^f(r)$, eq 2, at the individual locations r of the lipid chains. This follows from the ESR measuring process which extends over times on the order of 10^{-7} s and distinguishes labels with different order parameters by different signals. Up to six different signals could be distinguished in the presence of cytochrome c oxidase (Knowles et al., 1979), indicating the coherence length ξ to be of the order of 15 Å estimated previously. It needs hardly to be mentioned that ESR uses label groups and, therefore, does not detect the lipid order exactly.[5]

FA also measures the fast order parameter but as the average $\overline{S^f}$, since in the FA measuring process signals from labels with different order parameters are not distinguished. Apart from the fact that FA uses label groups as ESR, there are two additional points to be considered for such an interpretation of steady-state DPH-FA data. DPH molecules do not detect all kinds of conformational disorder, e.g., simple kinks, but sense predominantly the rigid-body order of the lipid chains (Hoffmann et al., 1981; Engel & Prendergast, 1981). This rigid-body order characterizes the rocking fluctuations of the entire lipid chains. The orientational order of the chains is a superposition of their conformational order and their rigid-body order. For this superposition, Petersen & Chan (1977) proposed the form of a product, $S = S_{\text{conformational}}S_{\text{rigid-body}}$. Thus DPH-FA in general detects only part of the orientational order. It has been shown experimentally, however, that over the so-called plateau region along the lipid chains the lipid conformation is predominantly all trans (Vogel & Jähnig, 1981), so that in this region the conformational order parameter is close to 1. The DPH-FA order parameter can therefore approximately be equated with the orientational order parameter of the lipid chain segments in the plateau region. The interpretation of steady-state FA measurements is further complicated by the fact that a superposition of static order and kinetic behavior is detected. Time-resolved FA experiments have shown, however, that the kinetic parameters, the fluorescence lifetime τ and the orientational relaxation time ϕ, do not vary appreciably with temperature or protein content (Kinoshita et al., 1981). The measured anisotropy values r_s can therefore be evaluated by use of the relation (Jähnig, 1979)

$$r_s = \frac{\frac{2}{5} - r_\infty}{1 + \tau/\phi} + r_\infty \tag{11a}$$

with a constant ratio τ/ϕ. For DPH in DMPC bilayers this ratio is $\tau/\phi \approx 8$. From the limiting anisotropy r_∞ the order parameter follows as (Jähnig, 1979)

$$\overline{S^f} = (\tfrac{5}{2}r_\infty)^{1/2} \tag{11b}$$

[4] In another model of lipid–protein interaction, in addition to unperturbed lipid and boundary lipid a third type of lipid was introduced, trapped lipid (Pink et al., 1981). As long as proteins are distributed homogeneously in the lipid bilayer, such trapped lipid may occur only at very high protein concentrations.

[5] Direct measurement of the boundary order parameter should be possible by attaching a spin-labeled hydrocarbon chain covalently to a protein (Davoust et al., 1979). This method applies analogously to the other experimental techniques.

In ^2H NMR, where the measuring process extends over times of the order of 10^{-4} s, the total orientational order parameter S is detected. This assignment of the order parameter measured by ^2H NMR is consistent with the observation of only one order parameter in the presence of protein in ^2H NMR. Since S is given by the product $\overline{S}^f S^s$ and since S^s decreases upon addition of protein (if it changes at all), the ^2H NMR order parameter may decrease even if the DPH-FA order parameter $\overline{S}^f$ increases.

In Raman spectroscopy, the intensity of the 1127-cm^{-1} band is proportional to the average number of trans bonds per chain, so that Raman yields a measure for the average conformational order of the lipid chains, which is only part of the orientational order as discussed for the FA technique. Concerning the averaging process, Raman detects an average over the instantaneous conformations of all chains. According to the laws of statistical mechanics, this ensemble average is equal to the average of the conformation of one chain over infinitely long times. Hence Raman detects the total conformational order and in this respect resembles more ^2H NMR than the fast techniques ESR and FA.

In addition to the introduction of fast, slow, and total orientational order in the last section, in this section we were compelled by the experimental techniques to further differentiate the lipid order by introducing the conformational order and the rigid-body order whose superposition yields the orientational order. Obviously, the distinction between fast, slow, and total order holds for any of them.

Evaluation of Experimental Results

The Raman results show that the conformational order of the lipid chains is decreased by melittin in the ordered phase but is increased slightly in the fluid phase. In contrast, the DPH anisotropy shows that the rigid-body order of the lipid chains remains constant in the ordered phase but is increased considerably by melittin in the fluid phase. This indicates that different types of lipid order must be distinguished and that a protein may influence each type of order differently. This point is further borne out by contrasting our Raman and DPH-FA results with the DMR results which show that melittin decreases the total orientational order in the fluid phase (Oldfield et al., 1981). Moreover, these experimental results for melittin are qualitatively the same for all other proteins investigated (Oldfield et al., 1981).[6] Hence, we conclude that the experimental data on lipid–protein interactions, in general, cannot be interpreted consistently in terms of an alteration of a single type of lipid order.

Without introducing any specific model, it is evident that if proteins in the fluid phase increase the total conformational order and decrease the total orientational order, a decrease of the total rigid-body order must be inferred. If, furthermore, the fast rigid-body order is increased by proteins, the slow rigid-body order must decrease. This implies that in the fluid phase proteins induce tilted preferred axes uniformly along the lipid chains, i.e., a tilt of the entire chains. This conclusion is in accord with the experimental finding obtained with specifically deuterated lipids that the protein-induced decrease of the ^2H NMR order parameter is rather uniform along the lipid chains (Seelig & Seelig, 1978; Rice et al., 1979). More exactly, the decrease of the ^2H NMR order parameter by protein is uniform over the plateau region and is more pronounced at the chain ends. This indicates a somewhat larger tilt angle at the chain ends. If furthermore the slight increase of the total conformational order is assigned to the region of the chain ends according to the arguments given above, this increase similarly has to be compensated by an increased tilt angle of the chain ends.

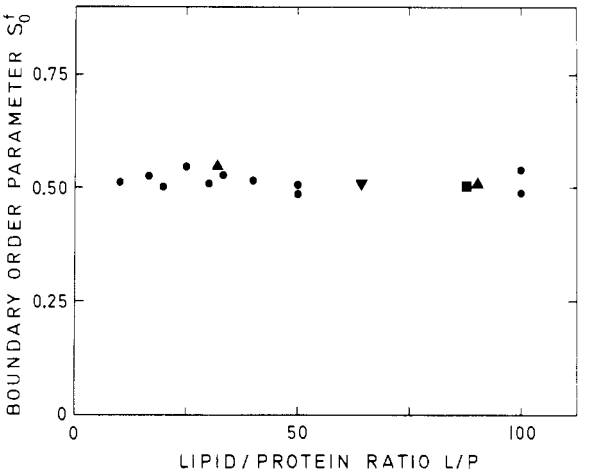

FIGURE 8: Boundary order parameter S^f_0 vs. lipid/protein ratio L/P for melittin in DMPC (●), Ca/Mg-ATPase in DMPC (▲) and DOPC (▼), and cytochrome *c* oxidase in DMPC (■) (in the latter case L/P is the effective lipid/protein ratio).

For the quantitative evaluation of the experimental results the model presented above is adopted, and the two parameters for lipid–protein interaction are determined. The evaluation is restricted to the fluid phase and the plateau region along the lipid chains. Here the DPH anisotropy yields approximately the fast orientational order parameter $\overline{S}^f$, the increase of the conformational order affecting only the chain end region. The data of Figure 4B at 35 °C can be evaluated for the boundary order parameter S^f_0 by using eq 11 and 9 and assuming R_L = 5 Å based on a lipid area of 60 Å^2, R_0 = 5 Å corresponding to one α helix for melittin,[7] and ξ = 15 Å implying a number of 30 boundary lipids within ξ. The result for S^f_0 for different lipid/protein ratios is shown in Figure 8. The boundary order parameter S^f_0 for an isolated melittin molecule is independent of the melittin concentration. This result is expected within the framework of our model and can, therefore, be regarded as a confirmation of the model. The mean value S^f_0 = 0.51 is higher than the unperturbed value S^f_u = 0.36, indicating that in the fluid phase melittin acts ordering on the fast orientational fluctuations of the lipid chains. Concerning the magnitude of S^f_0 it should be noted that the evaluation assumed all melittin molecules to be incorporated and to span the bilayer.

Let us briefly consider the result for the ordered phase. The decrease of the conformational order we attribute, in analogy

[6] The only exception is gramicidin A, which does not span the bilayer (in the closed-channel state) and increases the ^2H NMR order parameter like cholesterol (Rice & Oldfield, 1979).

[7] The description of melittin as a bilayer-spanning α helix deserves some justification. First, melittin was shown to adopt a conformation of 70% α-helix content upon association with a lipid bilayer (Vogel, 1981). The helical part may safely be identified with the membrane-incorporated hydrophobic part of melittin which comprises 20 of the 26 amino acid residues. Probably it contains two α-helical segments separated by a proline residue. Second, we have shown by polarized infrared absorption measurements on oriented samples that the helical part is inclined on the average at an angle of about 30° to the membrane normal (H. Vogel and F. Jähnig, unpublished results). This result is compatible with a conformation in which the two α-helical segments form a bent rod as found for the crystalline structure of melittin (Terwilliger et al., 1982), if, furthermore, one assumes that the rod is oriented on the average along the membrane normal. Hence, the membrane-incorporated part of melittin should span the bilayer.

to the fluid phase, to an increase of disorder at the chain ends, so that order parameters derived from DPH-FA still represent orientational order parameters of the plateau region. Since melittin does not alter the DPH anisotropy, we obtain from eq 9 $S^f_0 = S^f_u$ and from the data of Figure 4B at 15 °C and eq 11 $S^f_0 = 0.9$. This value indicates that the boundary order parameter of the plateau region varies on passing through the phase transition.

The result for melittin in the fluid phase may be compared with the result for other proteins. DPH-FA data for the system DMPC/(Ca/Mg)-ATPase are available, at two lipid/protein ratios L/P = 90 and 34 (Gomez-Fernandez et al., 1979). To evaluate them we proceed in the same way as for melittin so that the lack of Raman data for Ca/Mg-ATPase is unimportant. The only parameter which has to be changed is the protein radius for which we now assume $R_0 = 15$ Å. This value follows from the suggestion that the Ca/Mg-ATPase traverses the bilayer in eight helices corresponding to a molecular weight of 16 000 for the membrane part of the protein (MacLennon et al., 1980). The DPH-FA data at 35 °C then lead to $S^f_0 = 0.51$ and 0.54 for L/P = 90 and 34, respectively (Figure 8). Thus the boundary order parameter for the Ca/Mg-ATPase agrees well with that for melittin.

DPH-FA data are also available for Ca/Mg-ATPase in DOPC at L/P = 64 (Seelig et al., 1981). At 25 °C, i.e., again in the fluid phase, the unperturbed order parameter is $S^f_u = 0.18$ and the perturbed order parameter follows as $\overline{S^f} = 0.43$, using eq 11 with the appropriate values for DPH in DOPC, namely, $\tau = 7.7$ ns and $\phi = 1.84$ ns (Stubbs et al., 1981).[8] This leads to the boundary order parameter $S^f_0 = 0.51$. Although the unperturbed value is much lower in this case since DOPC at 25 °C is nearly 50 °C above its phase transition, the boundary value is again the same as above (Figure 8). This suggests that the boundary order parameter S^f_0 in contrast to the unperturbed order parameter S^f_u does not vary appreciably upon approaching the phase transition.

Another example for which DPH-FA data exist is the system DMPC/cytochrome *c* oxidase (Kawato et al., 1980). At 35 °C and L/P = 176, the DPH order parameter results as $\overline{S^f} = 0.43$, the unperturbed value being $S^f_u = 0.36$ as above. Two subunits of cytochrome *c* oxidase are supposed to traverse the bilayer with eight α helices each (Prochaska et al., 1980). The eight helices correspond to a radius $R_0 = 15$ Å as in the case of the Ca/Mg-ATPase, and the presence of two subunits can be accounted for by using an effective lipid/protein ratio of 88 instead of 176. Then the boundary order parameter results as $S^f_0 = 0.51$. Thus for the three examples of proteins considered, the boundary order parameter is found to be the same, with a value of about 0.51, suggesting a uniform effect of different proteins on lipid order.

For the determination of the boundary tilt angle θ^s_0, ^{2}H NMR data are required. Unfortunately, for melittin such data are not available except for the remark that melittin acts on the lipids in the same way as other proteins. The protein/lipid systems investigated by ^{2}H NMR include Ca/Mg-ATPase in DMPC (Rice et al., 1979) and DOPC (Seelig et al., 1981) and cytochrome *c* oxidase in POPC (Seelig & Seelig, 1978), DMPC (Kang et al., 1979), and P(PO)PC (Paddy et al., 1981). The uniform result is that the ^{2}H NMR order parameter is decreased by 15% for an effective lipid/protein ratio of 60. This again suggests a uniform effect of different proteins on lipid order. We determine the boundary tilt angle θ^s_0 for a representative example assuming a 15% decrease of the total orientational order parameter S in the plateau region for both Ca/Mg-ATPase and cytochome *c* oxidase in DMPC at L/P = 60 (effective value for cytochrome *c* oxidase) and 35 °C. For the unperturbed order parameter we use the value $S^f_u = 0.36$ as above which is in good agreement with the ^{2}H NMR result for DPPC at segment 9–10 and the corresponding temperature on a reduced temperature scale (Seelig & Seelig, 1974). The 15% decrease leads to $S = 0.30$. The spatially averaged fast order parameter for the present conditions is $\overline{S^f} = 0.44$ according to eq 9 and the DPH-FA result $S^f_0 = 0.51$. The slow orientational order parameter then follows from eq 8 as $S^s = 0.68$. Since this value deviates considerably from 1, a finite boundary tilt angle θ^s_0 must exist. The value of θ^s_0 according to eq 10 depends upon the coherence length λ. Because λ is not well-known, we plotted in Figure 9 the result for θ^s_0 as a function of λ. With increasing λ, θ^s_0 decreases and levels off at a value of about 20°. A lower limit for λ is $\xi = 15$ Å as mentioned, so that θ^s_0 turns out to lie in the range between 20° and 30°.

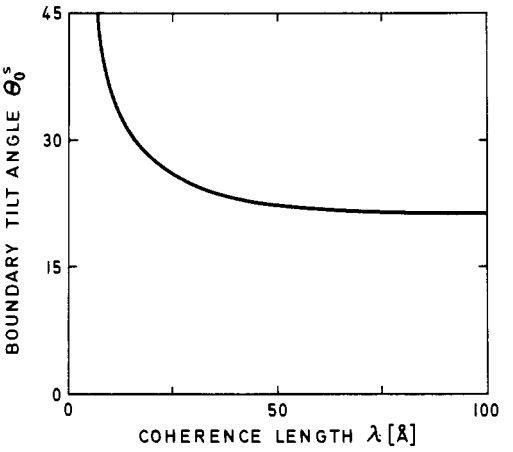

FIGURE 9: Boundary tilt angle θ^s_0 vs. lipid coherence length λ for Ca/Mg-ATPase or cytochrome *c* oxidase in DMPC.

It should be remembered that this evaluation is based on the equalization of the DPH-FA order parameter with the fast orientational order parameter in the plateau region. This is certainly an approximation which has to be improved in future work. On the one hand, this approximation may imply an underestimate of the effect of proteins, i.e., of the boundary values S^f_0 and θ^s_0, in the plateau region since the increase of the conformational order observed by Raman is assigned completely to the chain end region. On the other hand, this may represent an overestimate, if for unknown reasons the DPH anisotropy is more strongly affected by protein than the lipid fast rigid-body order.

Conclusion

In any attempt to understand the effect of proteins on lipid order in membranes, different kinds of lipid order must be distinguished. In the present paper, this is demonstrated for the conformational order of the lipid chains measured by Raman spectroscopy and the rigid-body orientational order measured by DPH-FA. These two kinds of order are affected

[8] Caution is warranted concerning the values given for S^f_u and $\overline{S^f}$, because they were not derived from one set of experimental data. $\overline{S^f}$ was obtained from the DPH anisotropy of DOPC/(Ca/Mg)-ATPase measured by Seelig et al. (1981). For the determination of S^f_u, however, their data for pure DOPC could not be used, since they lead to a negative value for r_∞. The origin of this inconsistency lies in the rather low values of the DPH anisotropy of DOPC obtained by Seelig et al. (1981) compared to those of other groups (Lakowicz et al., 1979; Stubbs et al., 1981). We, therefore, used the result of these groups to determine S^f_u, as done also by Seelig et al. (1981).

differently by melittin. In addition, the order parameter measured by ^2H NMR was taken into consideration, and it was concluded that the total orientational order should be divided into fast and slow components. The fast order involves the local fluctuations of lipid chain orientation and is increased by protein, the slow order involves the fluctuations of the preferred axes of orientation (as the lipids undergo lateral diffusion) and is decreased by protein.

The experimental data were evaluated quantitatively within a continuum model of lipid–protein interaction for the boundary values of the fast order parameter, S^f_0, and of the tilt angle of the preferred axes, θ^s_0. In the fluid phase, S^f_0 was found to be higher than the unperturbed order parameter. Moreover, the same value for S^f_0 was obtained for melittin, Ca/Mg-ATPase, and cytochrome *c* oxidase. This similarity among proteins also seems to hold for the boundary tilt angle. Within the limits of the uncertainty in the lipid coherence length λ, θ^s_0 lies between 20° and 30°.

The similarity among different proteins may have its origin in the common conformation of their membrane part which is predominantly α helical for the proteins treated here (Vogel, 1981; MacLennon et al., 1980; Prochaska et al., 1980). In the fluid lipid phase, an α helix due to its rigidity restricts the fast rigid-body fluctuations of the lipid chains leading to an increased boundary order parameter S^f_0. On the other hand, the uneven surface of an α helix may induce a tilt of the preferred axes of chain orientation, i.e., a finite boundary tilt angle θ^s_0.

Acknowledgments

We thank Keith Wright for a critical reading of the manuscript.

References

Brown, M. F., Seelig, J., & Häberlen, U. (1979) *J. Chem. Phys. 70*, 5045.

Chapman, D., Cornell, B. A., Eliasz, A. W., & Perry, A. (1977) *J. Mol. Biol. 113*, 517.

Curatolo, W., Verma, S. P., Sakura, J. D., Small, D. M., Shipley, G. G., & Wallach, D. F. H. (1978) *Biochemistry 17*, 1802.

Davoust, J., Schoot, B. M., & Devaux, P. F. (1979) *Proc. Natl. Acad. Sci. U.S.A. 76*, 2755.

Dawson, C. R., Drake, A. F., Helliwell, J., & Hider, R. C. (1978) *Biochim. Biophys. Acta 510*, 75.

de Gennes, P. G. (1974) *The Physics of Liquid Crystals*, p 84, Oxford University Press, London.

Engel, L. W., & Prendergast, F. G. (1981) *Biochemistry 20*, 7338.

Galla, H. J., Hartmann, W., & Sackmann, E. (1978) *Ber. Bunsenges. Phys. Chem. 82*, 918.

Gomez-Fernandez, J. C., Goni, F. M., Bach, D., Restall, C., & Chapman, D. (1979) *FEBS Lett. 98*, 224.

Heyn, M. P., Cherry, R. J., & Dencher, N. A. (1981) *Biochemistry 20*, 840.

Hoffmann, W., Pink, D. A., Restall, C., & Chapman, D. (1981) *Eur. J. Biochem. 114*, 585.

Jähnig, F. (1979) *Proc. Natl. Acad. Sci. U.S.A. 76*, 6361.

Jähnig, F. (1981) *Biophys. J. 36*, 329, 347.

Jähnig, F., Harlos, K., Vogel, H., & Eibl, H. (1979) *Biochemistry 18*, 1459.

Janiak, M. J., Small, D. M., & Shipley, G. G. (1976) *Biochemistry 15*, 4575.

Kang, S. Y., Gutowsky, H. S., Hsung, J. C., Jacobs, R., King, T. E., Rice, D., & Oldfield, E. (1979) *Biochemistry 18*, 3257.

Kawato, S., Kinoshita, K., Jr., & Ikegami, A. (1977) *Biochemistry 16*, 2319.

Kawato, S., Ikegami, A., Yoshida, S., & Orii, Y. (1980) *Biochemistry 19*, 1598.

Kimelman, D., Tecoma, E. S., Wolber, P. K., Hudson, B. S., Wickner, W. T., & Simoni, R. D. (1979) *Biochemistry 18*, 5874.

Kinoshita, K., Jr., Kawato, S., Ikegami, A., Yoshida, S., & Orii, Y. (1981) *Biochim. Biophys. Acta 647*, 7.

Knowles, P. F., Watts, A., & Marsh, D. (1979) *Biochemistry 18*, 4480.

Lakowicz, J. R., Prendergast, F. G., & Hogen, D. (1979) *Biochemistry 18*, 508.

Lavialle, F., Levin, I. W., & Mollay, C. (1980) *Biochim. Biophys. Acta 600*, 62.

Lentz, B. R., Barenholz, Y., & Thompson, T. E. (1976) *Biochemistry 15*, 4529.

Lippert, J. L., Lindsay, R. M., & Schultz, R. (1980) *Biochim. Biophys. Acta 599*, 32.

MacLennon, D. H., Reithmeier, R. A. F., Shoshan, V., Campbell, K. P., LeBel, D., Herrmann, T. R., & Shamoo, A. E. (1980) *Ann. N.Y. Acad. Sci. 358*, 138.

Mollay, C. (1976) *FEBS Lett. 64*, 65.

Oldfield, E., Janes, N., Kinsey, R., Kintanar, A., Lee, R. W. K., Rothgeb, T. M., Schramm, S., Skarjune, R., Smith, R., & Tsai, M.-D. (1981) *Biochem. Soc. Trans. 45*, 155.

Owicki, J. C., Springgate, M. W., & McConnell, H. M. (1978) *Proc. Natl. Acad. Sci. U.S.A. 75*, 1616.

Paddy, M. R., Dahlquist, F. W., Davis, J. H., & Bloom, M. (1981) *Biochemistry 20*, 3152.

Petersen, N. O., & Chan, S. I. (1977) *Biochemistry 16*, 2657.

Pink, D. A., Georgallas, A., & Chapman, D. (1981) *Biochemistry 20*, 7152.

Prochaska, L., Bisson, R., & Capaldi, R. A. (1980) *Biochemistry 19*, 3174.

Rice, D. M., & Oldfield, E. (1979) *Biochemistry 18*, 3272.

Rice, D. M., Meadows, M. D., Scheinman, A. O., Goni, F. M., Gomez-Fernandez, J. C., Moscarello, M. A., Chapman, D., & Oldfield, E. (1979) *Biochemistry 18*, 5893.

Seelig, A., & Seelig, J. (1974) *Biochemistry 13*, 4839.

Seelig, A., & Seelig, J. (1978) *Hoppe Seyler's Z. Physiol. Chem. 359*, 1747.

Seelig, J., Tamm, L., Hymel, L., & Fleischer, S. (1981) *Biochemistry 20*, 3922.

Sessa, G., Freer, J. H., Colacicco, G., & Weissmann, G. (1969) *J. Biol. Chem. 244*, 3575.

Stubbs, C. D., Kouyama, T., Kinoshita, K., Jr., & Ikegami, A. (1981) *Biochemistry 20*, 4257.

Susi, H., Sampugna, J., Hampson, J. W., & Ard, J. S. (1979) *Biochemistry 18*, 297.

Terwilliger, T. C., Weissman, L., & Eisenberg, D. (1982) *Biophys. J. 37*, 353.

Vogel, H. (1981) *FEBS Lett. 134*, 37.

Vogel, H., & Jähnig, F. (1981) *Chem. Phys. Lipids 29*, 83.

Weidekamm, E., Bamberg, E., Brdiczka, D., Wildermuth, G., Macco, F., Lehmann, W., & Weber, R. (1977) *Biochim. Biophys. Acta 464*, 442.

Wolber, P. K., & Hudson, B. S. (1979) *Biophys. J. 28*, 197.

Wolber, P. K., & Hudson, B. S. (1981) *Biochemistry 20*, 2800.